ELSEVIER

Journal of Organometallic Chemistry 538 (1997) 119–128

Journal of Organometallic Chemistry

Trisimidazole complexes of ruthenium and osmium

Sarah Elgafi, Leslie D. Field *, Barbara A. Messerle, Irmi E. Buys, Trevor W. Hambley

School of Chemistry, University of Sydney, Sydney, N.S.W. 2006, Australia

Received 24 September 1996; revised 7 November 1996

Abstract

The preparation and characterisation of ruthenium(II) and osmium(II) complexes with the trisimidazole ligands tris(*N*-methylimidazol-2-yl)methanol (**1a**) ($(mim)_3COH$) and tris(*N*-ethoxymethylimidazol-2-yl)methanol (**1b**) ($(emim)_3COH$) are reported (mim = *N*-methylimidazol-2-yl, emim = *N*-ethoxymethylimidazol-2-yl). The complex $[\{RuCl(PPh_3)_2((mim)_3COH)\}^+Cl^-]$ (**2**) was formed by the reaction of $(mim)_3COH$ with $[RuCl_2(PPh_3)_4]$. The complexes $[\{Ru(PPh_3)(CO)H((mim)_3COH)\}^+Cl^-]$ (**3a**) and $[\{Ru(PPh_3)(CO)H((emim)_3COH)\}^+Cl^-]$ (**3b**) were formed by the reaction of $(mim)_3COH$ or $(emim)_3COH$ (respectively) with $[Ru(PPh_3)_3HCl(CO)]$. Likewise, the reaction of $(mim)_3COH$ or $(emim)_3COH$ (respectively) with $[Os(PPh_3)_3HCl(CO)]$ formed $[\{Os(PPh_3)(CO)H((mim)_3COH)\}^+Cl^-]$ (**4a**) and $[\{Os(PPh_3)(CO)H((emim)_3COH)\}^+Cl^-]$ (**4b**). The ruthenium monohydride complex $[\{Ru(PPh_3)(CO)H((mim)_3COH)\}^+Cl^-]$ (**3a**) adds to the terminal C–H bond of phenylacetylene to form the vinyl complex $[\{Ru(PPh_3)(CO)(CH{=}CHPh)((mim)_3COH)\}^+Cl^-]$ (**5**). The air-stable complexes were characterised by multinuclear NMR spectroscopy and **2** and **3b** were characterised by X-ray crystallography. Crystals of **2**, $C_{49}H_{46}N_6OP_2RuCl_2$, *M* 968.87, are triclinic, space group $P\bar{1}$, $a = 12.011(5)$, $b = 13.342(3)$, $c = 16.554(6)$ Å, $\alpha = 89.26(3)°$, $\beta = 76.94(3)°$, $\gamma = 77.43(3)°$, $Z = 2$. Crystals of **3b**, $C_{38}H_{44}N_6O_5PRuCl$, *M* 832.30, are triclinic, space group $P\bar{1}$, $a = 12.759(3)$, $b = 13.017(2)$, $c = 13.167(4)$ Å, $\alpha = 87.65(2)°$, $\beta = 64.09(2)°$, $\gamma = 88.82(2)°$, $Z = 2$.

Keywords: Imidazole; Ruthenium; Osmium; Trisimidazole; Polyimidazole; NOESY

1. Introduction

Imidazole-based ligands constitute a relatively small portion of the class of nitrogen-containing heterocyclic ligands. A number of multidentate ligands based on the imidazole ring system have been prepared previously and these ligands have been employed with a range of metals, predominantly Zn [1–3], Fe [4–7], Co [1,2] and Cu [8–12]. Polydentate imidazole-based ligands have found their greatest application in the area of enzyme mimicry. The impetus for the study of imidazole-based ligands is that it is the aromatic chelating unit in histidine and histidine serves as a natural ligand bound to metals in many biological catalytic (enzymatic) processes. Consequently, polyimidazole ligand systems have been used to model compounds related to non-heme metalloproteins, particularly carbonic anhydrase (a zinc containing metalloenzyme), hemerythrin and hemocyanin (dioxygen transport proteins) [13]. Polyimidazole ligands have also been used in the study of copper complexes as synthetic analogues for cuproprotein active sites [8,9]. Little is known of the coordination chemistry of polyimidazole ligands to other metals, with the exception of a small number of palladium [14], platinum [15] and ruthenium [16] complexes.

In this paper we report the synthesis and characterisation of ruthenium and osmium complexes containing the trisimidazole ligands, tris(*N*-methylimidazol-2-yl)methanol (**1a**) ($(mim)_3COH$) and tris(*N*-ethoxymethylimidazol-2-yl)methanol (**1b**) ($(emim)_3COH$). The complexes $[\{RuCl(PPh_3)_2((mim)_3COH)\}^+Cl^-]$ (**2**), $[\{Ru(PPh_3)(CO)H((mim)_3COH)\}^+Cl^-]$ (**3a**), $[\{Ru(PPh_3)(CO)H((emim)_3COH)\}^+Cl^-]$ (**3b**), $[\{Os(PPh_3)(CO)H((mim)_3COH)\}^+Cl^-]$ (**4a**), and $[\{Os(PPh_3)(CO)H((emim)_3COH)\}^+Cl^-]$ (**4b**) have been completely characterised by multinuclear NMR spec-

* Corresponding author.

PII S0022-328X(96)06910-0

troscopy, and **2** and **3b** have been structurally characterised by X-ray crystallography.

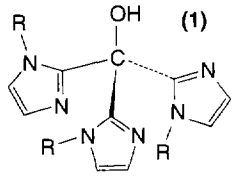

(1)

a R = CH_3 ($(mim)_3COH$)
b R = $CH_2OCH_2CH_3$ ($(emim)_3COH$)

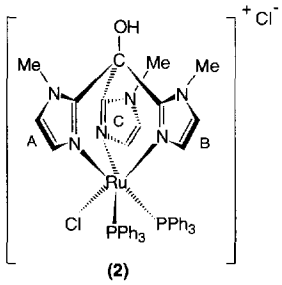

(2)

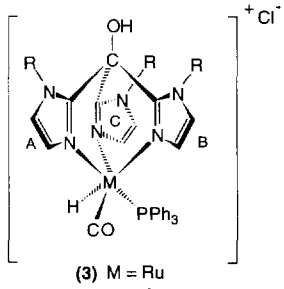

(3) M = Ru
(4) M = Os

2. Results and discussion

The ligands **1a** ($(mim)_3COH$) and **1b** ($(emim)_3COH$) were synthesised using modifications of literature methods [17]. The charged species $[\{RuCl(PPh_3)_2((mim)_3COH)\}^+Cl^-]$ (**2**) was formed as a yellow crystalline solid by the reaction of $[RuCl_2(PPh_3)_4]$ with $(mim)_3COH$ (**1a**). The complex is analogous to the known tris(pyrazol-1-yl)borate (TPB) and tris(pyrazol-1-yl)methane (TPM) ruthenium complexes: $[RuCl(PPh_3)_2(TPB)]$ [18], $[RuCl(PPh_3)_2(TPM)]^+$ [19], $[Ru(TPM)(OH_2)_3]^{2+}$ [20], and $[RuCl(COD)(TPM)]^+$ [21].

The air-stable complex $[\{Ru(PPh_3)(CO)H((mim)_3COH)\}^+Cl^-]$ (**3a**) was formed by the reaction of $(mim)_3COH$ (**1a**) with $[Ru(PPh_3)_3HCl(CO)]$, and $[\{Ru(PPh_3)(CO)H((emim)_3COH)\}^+Cl^-]$ (**3b**) was formed by reaction of $(emim)_3COH$ (**1b**) with $[Ru(PPh_3)_3HCl(CO)]$. The complex **3b** is air-stable and was characterised by single crystal X-ray diffraction. Analogous poly(pyrazol-1-yl)borate complexes $[Ru(\eta^3\text{-}HB(pyrazol\text{-}1\text{-}yl)_3)(PPh_3)(CO)(H)]$ have been described elsewhere [22], and these were synthesised by the reaction of tris(pyrazol-1-yl)borates with $[Ru(PPh_3)_3HCl(CO)]$.

The air-stable osmium(II) complexes $[\{Os(PPh_3)(CO)H((mim)_3COH)\}^+Cl^-]$ (**4a**) and $[\{Os(PPh_3)(CO)H((emim)_3COH)\}^+Cl^-]$ (**4b**) were formed by the reaction of $[Os(PPh_3)_3HCl(CO)]$ with **1a** ($(mim)_3COH$) and **1b** ($(emim)_3COH$) respectively. The complexes **2**, **3a**, **3b**, **4a** and **4b** were fully characterised by NMR spectroscopy. For the compounds **3a**, **3b**, **4a** and **4b** with one metal bound hydride, the stereospecific assignment of the ^1H NMR spectra was achieved using ^1H NOESY NMR spectra. The two imidazolyl rings closest to the metal bound hydride show strong NOESY cross peaks between the resonances of the hydride and protons of two of the imidazolyl rings (labelled A and C in Fig. 1). The NOESY cross peaks {hydride ⇔ $H4_A$} and {hydride ⇔ $H4_C$} are approximately equal in intensity, which indicates that the hydride is approximately equally distant from the two imidazolyl rings, consistent with the octahedral geometry of the system.

The complexes **2**, **3a**, **3b**, **4a** and **4b** are chiral at the metal centre and in the ^1H NMR spectra of **3b** and **4b**, where the trisimidazole ligand was $(emim)_3COH$, the methylene protons N–CH_2–O are diastereotopic and give rise to separate resonances in their ^1H NMR spectra.

At room temperature the ^1H, ^{31}P and ^{13}C NMR spectra of the complexes **2**, **3a**, **3b**, **4a** and **4b** show that the three phenyl rings of the metal bound triphenylphosphine ligands are equivalent. For complex **2**, the ^{31}P resonance broadens and splits into two signals at low temperature [coalescence of ^{31}P resonances ($\Delta\nu$ = 125 Hz) was observed at 225 K, 400 MHz; this corresponds to an approximate barrier of $\Delta G^{\neq}_{225\,K}$ = 40.2 kJ mol^{-1}]. Similarly, the ^1H signals for the imidazolyl rings split to show three non-equivalent imidazolyl rings at low temperature. The dynamic behaviour of **2** is consistent with a slowing of the rotation of the triphenylphosphine groups about the metal–P bonds. Restricted rotation is not unexpected with two bulky triphenylphosphine in *cis* coordination sites. The motion of the triphenylphosphine ligands must freeze to conformations where the PPh_3 groups are non-equivalent, and this probably involves interleaving or 'cog-wheeling' of

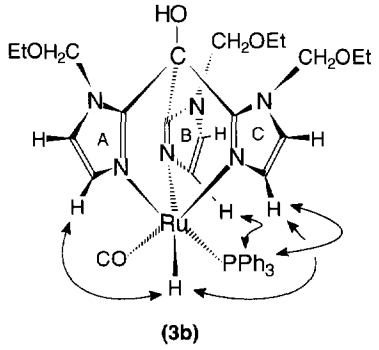

(3b)

Fig. 1. Structure of **3b** indicating strong NOESY interactions observed.

the phenyl substituents on the phosphorus donors (see for example Ref. [23]).

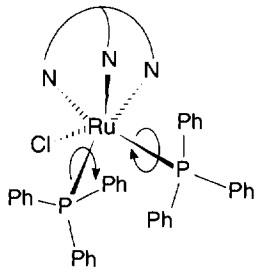

2.1. X-ray structures of 2 and 3b

The structures of the ruthenium complexes **2** and **3b** were obtained by single crystal structure analysis. Both $[\{RuCl(PPh_3)_2((mim)_3COH)\}^+Cl^-]$ (**2**) and $[\{Ru(PPh_3)(CO)H((emim)_3COH)\}^+Cl^-]$ (**3b**) crystallise as air-stable yellow prisms from methanol. The crystal data parameters for each complex are summarised in Table 1. Views of the cations **2** and **3b** are shown in Figs. 2 and 3 respectively. The bond lengths and angles for the inner coordination sphere are listed in Tables 2 and 3 respectively.

Complexes **2** and **3b** are both essentially octahedral about the central ruthenium atom. There is some distortion from ideal octahedral geometry and this results from the constraints imposed on the three imidazolyl nitrogen donor atoms by the trisimidazole ligand architecture. In complex **2**, the angle between two coordinated nitrogen atoms and ruthenium varies between 79 and 86°, and in compound **3b** the angles are between 81 and 83°. This distortion is reflected throughout the structure, with corresponding deviations from octahedral geometry in the bite angles between the phosphorus

Table 1
Crystallographic data for $[\{RuCl(PPh_3)_2((mim)_3COH)\}^+Cl^-]$ (**2**) and $[\{Ru(PPh_3)(CO)H((emim)_3COH)\}^+Cl^-]$ (**3b**)

	2	**3b**
Chemical formula	$C_{49}H_{46}N_6OP_2RuCl_2$	$C_{38}H_{44}N_6O_5PRuCl$
FW (g mol^{-1})	968.87	832.30
Crystal system	triclinic	triclinic
Crystal colour	yellow	colourless
Crystal habit	prism	prism
Crystal dimensions	0.25 × 0.20 × 0.45	0.11 × 0.12 × 0.15
T (°C)	20	21
Space group	$P\bar{1}$	$P\bar{1}$
V (Å^3)	2520	1965.33
a (Å)	12.011(5)	12.759(3)
b (Å)	13.342(3)	13.017(2)
c (Å)	16.554(6)	13.167(4)
α (°)	89.26(3)	87.65(2)
β (°)	76.94(3)	64.09(2)
γ (°)	77.43(3)	88.82(2)
Z	2	2
D_{calc} (g cm^{-3})	1.677	1.406
θ range (°)	$1 < \theta < 25$	$1 < \theta < 2.5$
Scan type	ω–$2/3\theta$	ω–$1/3\theta$
No. of reflections measured	8614	5284
No. of observed reflections	6657	3369
Criterion of observed	$I > 2.5\sigma(I)$	$I > 2.5\sigma(I)$
Range of *h*, *k*, *l*	$-14 \rightarrow 14$, $-15 \rightarrow 15$, $0 \rightarrow 19$	$-12 \rightarrow 12$, $-12 \rightarrow 12$, $0 \rightarrow 12$
Number of variables	635	469
Absorption coefficients (cm^{-1})	5.3	5.57
R *	0.0478	0.044
R_w	0.0538	0.044
Shift/e.s.d.	0.081	0.03
λ (Å)	0.71069	0.71069
Radiation source	Mo Kα	Mo Kα
Diffractometer	Enraf–Nonius CAD4-F	Enraf–Nonius CAD4-F
Monochromator	graphite	graphite
Refinement	SHELX-76	SHELX-76
Data reduction	Enraf–Nonius SDP	Enraf–Nonius SDP
Solution	SHELX-86	SHELX-86
H atoms	calc.	calc.

* $R = \Sigma(||F_o| - |F_c||)/\Sigma|F_o|$, $R_w = (\Sigma w(|F_o| - |F_c|)^2/\Sigma wF_o^2)^{1/2}$.

and nitrogen atoms bound to ruthenium, as well as in the angle between the chloride and carbonyl groups.

There is also some distortion in the tetrahedral geometry about the apical carbon atom of the tridentate ligand. For both molecules, the imidazolyl subunits are compressed slightly with reduced bond angles for $C_{imidazolyl}-C_{bridghead}-C_{imidazolyl}$ of 102°, 107° and 111° for compound **2** (Fig. 2(b)) and 106°, 105° and 110° for compound **3b** (Fig. 3(b)). The corresponding external angles, which include the oxygen atom bound to the bridgehead carbon atom ($O-C_{bridgehead}-C_{imidazolyl}$), are all expanded with angles ranging from 110°–113° for both **2** and **3b**.

The lengths of the Ru–N bonds are comparable in complexes **2** and **3b**, with those of **3b** being slightly longer than those of complex **2** (Table 2). The length of the Ru–N bond, where N is *trans* to Cl in **2**, is slightly shorter (2.062(3) Å) than the other two Ru–N bonds (2.123(3) and 2.137(4) Å). In complex **3b** the three Ru–N bonds are all of comparable length, at 2.151(6), 2.152(5) and 2.169(5) Å. The Ru–P bond in complex **3b** is slightly shorter at 2.295(2) Å than the two Ru–P bond

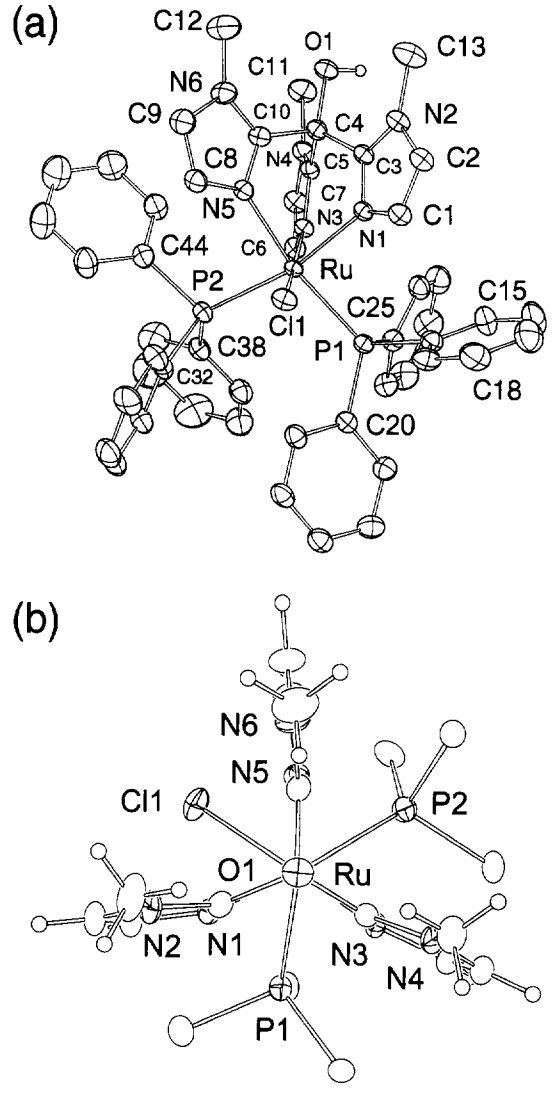

Fig. 2. ORTEP of $[\{RuCl(PPh_3)_2((mim)_3COH)\}^+ Cl^-]$ (**2**); 30% thermal ellipsoids are shown for the non-hydrogen atoms; hydrogen atoms have an arbitrary radius of 0.1 Å. (a) Numbering scheme; (b) view of **2** down the axis through the central carbon of the $(mim)_3COH$ ligand and the ruthenium atom.

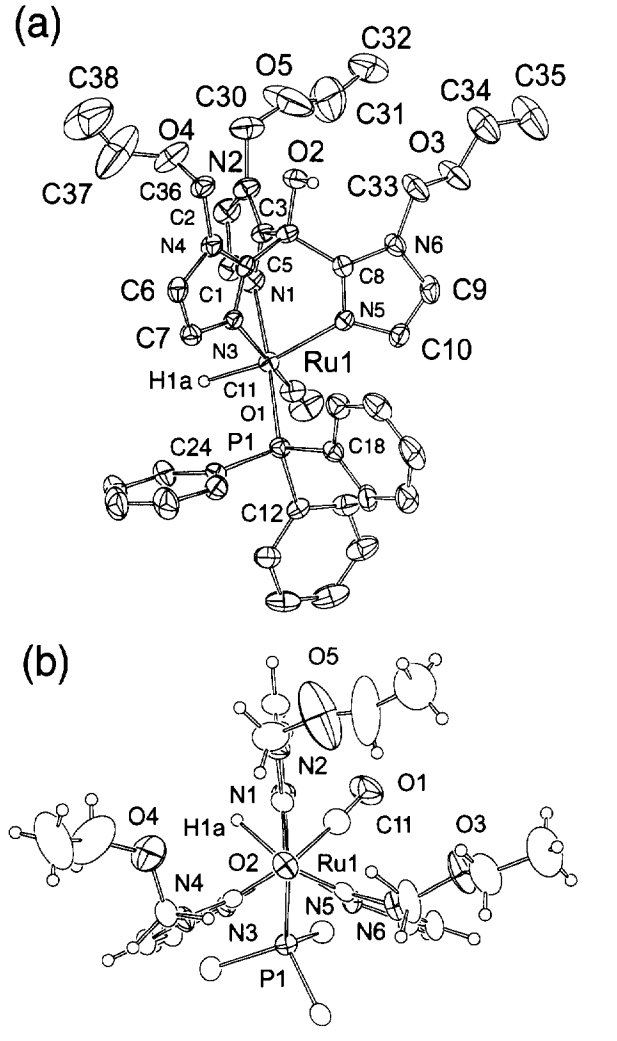

Fig. 3. ORTEP of $[\{Ru((emim)_3COH)(PPh_3)(CO)H\}^+ Cl^-]$ (**3b**); 20% thermal ellipsoids are shown for the non-hydrogen atoms; hydrogen atoms have an arbitrary radius of 0.1 Å. (a) Numbering scheme; (b) view of **3b** down the axis through the central carbon of the $(emim)_3COH$ ligand and the ruthenium atom.

Table 2
Core bond lengths (Å) in **2** and **3b** [a]

Atom pairs (**2**)	Bond lengths in **2**	Atom pairs (**3b**)	Bond lengths in **3b**
Ru–Cl	2.420(1)		
Ru–P1	2.344(1)	Ru–CO	1.814(8)
Ru–P2	2.371(1)	Ru–P1	2.295(2)
Ru–N1	2.123(3)	Ru–N1	2.151(6)
Ru–N5	2.137(4)	Ru–N3	2.152(5)
Ru–N3	2.062(3)	Ru–N5	2.169(5)

[a] Atom numbering as in Figs. 2 and 3.

Table 3
Core bond angles (°) in **2** and **3b** [a]

Atoms (**2**)	Bond angles in **2**	Atoms (**3b**)	Bond angles in **3b**
P1–Ru–P2	102.4(0)	P1–Ru–CO	92.1(2)
Cl–Ru–P1	91.6(0)		
Cl–Ru–P2	95.9(0)		
N1–Ru–N3	86.0(1)	N1–Ru–N5	82.8(2)
N1–Ru–N5	79.4(1)	N1–Ru–N3	81.9(2)
N5–Ru–N3	85.7(1)	N5–Ru–N3	81.8(2)
N1–Ru–P1	90.0(1)	N1–Ru–CO	91.1(3)
N1–Ru–P2	167.2(1)	N1–Ru–P1	175.9(2)
N1–Ru–Cl	86.9(1)		
N3–Ru–P1	94.3(1)	N5–Ru–CO	100.8(3)
N3–Ru–P2	89.8(1)	N5–Ru–P1	99.1(3)
N3–Ru–Cl	170.7(1)		
N5–Ru–P1	169.3(1)	N3–Ru–CO	172.2(3)
N5–Ru–P2	88.2(1)	N3–Ru–P1	94.8(1)
N5–Ru–Cl	169.3(1)		
C5–C4–C3	111.4(4)	C8–C4–C3	105.6(5)
C10–C4–C3	101.8(3)	C5–C4–C3	105.4(5)
C10–C4–C5	106.9(3)	C8–C4–C5	110.1(5)
O–C4–C3	113.1(4)	O–C4–C3	111.4(5)
O–C4–C10	110.2(4)	O–C4–C5	112.0(5)
O–C4–C5	112.7(3)	O–C4–C8	112.0(5)

[a] Atom numbering as in Figs. 2 and 3.

lengths in complex **2** (2.344(1) and 2.371(1) Å). The imidazolyl rings are slightly twisted (canted) relative to the octahedral axes in both complexes **2** and **3b** (Fig. 2(b) and Fig. 3(b)). In complex **3b**, the imidazolyl rings A and B are twisted from the line joining the central metal atom and the apical carbon by as much as 10° (see Table 4).

The complex $[\{RuCl(PPh_3)_2((mim)_3COH)\}^+Cl^-]$ (**2**) is analogous to the tris(pyrazol-1-yl)borate (TPB) ruthenium $[RuCl(PPh_3)_2(TPB)]$ [18] and tris(pyrazol-1-yl)alkane (TPM) ruthenium $[\{RuCl(PPh_3)_2(TPM)\}^+Cl^-]$ [19] complexes described elsewhere. The slight distortion from octahedral geometry observed for **2** is also observed in the structure of $[\{RuCl(PPh_3)_2(TPM)\}^+Cl^-]$ [19] where the imidazolyl rings are apparently compressed slightly giving N–Ru–N bond angles of 78.4(2)°, 86.4(2)° and 87.2(2)°. The Ru–N bond lengths found in $[\{RuCl(PPh_3)_2(TPM)\}^+Cl^-]$ (2.083(6), 2.117(6) and 2.126(6) Å) are similar to those of **2** (Table 1) with the Ru–N bond *trans* to the metal bound

Table 4
Torsion angles in **2** and **3b**

Atoms (**2**)	Bond angles in **2**	Atoms (**3b**)	Bond angles in **3b**
Ru–N3–C5–C4	5.9(4)	Ru–N5–C8–C4	10.4(8)
Ru–N1–C3–C4	−3.0(4)	Ru–N1–C3–C4	1.8(9)
Ru–N5–C10–C4	−3.8(4)	Ru–N3–C5–C4	−4.4(8)
N2–C3–C4–O1	21.5(6)	N2–C3–C4–O2	−2(1)
N6–C10–C4–O1	−7.7(6)	N4–C5–C4–O2	9.1(9)
N4–C5–C4–O1	−10.9(6)	N6–C8–C4–O2	−10.2(9)

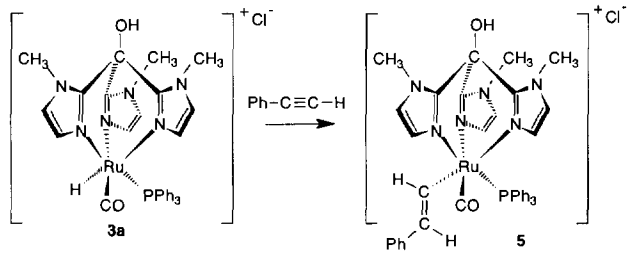

Scheme 1.

chloride being the shortest in both complexes. The Ru–P bond lengths are also comparable for $[\{RuCl(PPh_3)_2((mim)_3COH)\}^+Cl^-]$ (**2**), $[\{RuCl(PPh_3)_2(TPM)\}^+Cl^-]$ and $[RuCl(PPh_3)_2(TPB)]$ all fall within the range 2.33 to 2.37 Å. In **2**, however, the Ru–Cl bond (2.420(1) Å) is slightly longer than the corresponding Ru–Cl bonds in $[\{RuCl(PPh_3)_2(TPM)\}^+Cl^-]$ (2.402(2) Å) and $[RuCl(PPh_3)_2(TPB)]$ (2.409(3) Å).

2.2. Reaction of $[\{Ru(Ph_3)(CO)H((mim)_3COH)\}^+Cl^-]$ (3a) with phenylacetylene

The ruthenium monohydride complex $[\{Ru(PPh_3)(CO)H((mim)_3COH)\}^+Cl^-]$ (**3a**) adds to the terminal C–H bond of phenylacetylene to form the ruthenium alkenyl complex $[\{Ru(PPh_3)(CO)(CH=CHPh)((mim)_3COH)\}^+Cl^-]$ (**5**) (Scheme 1).

The product alkenyl ruthenium species is stable to air, and was fully characterised by multinuclear NMR. The reaction is analogous to the formation of $[Ru(PPh_3)(CO)(CR=CHR)(TPB)]$ from $[Ru(PPh_3)(CO)H(TPB)]$, described by Hill and coworkers [24]. The coordinated alkenyl groups in related complexes, derived from the reaction between $[Ru(PPh_3)_3HCl(CO)]$ and acetylenes, are known to couple with CS_2, pyrazoles, CO and carboxylates [25]. Metal-bound vinyl groups are also known to couple to acetylenes to form butadienyl complexes [26].

The metal vinyl complex **5** was also synthesised using an alternative approach, by displacing triphenylphosphine and chloride from $[RuCl(PPh_3)_2(CO)(trans\text{-}CH=CHPh)]$ with $(mim)_3COH$ to form $[\{Ru(PPh_3)(CO)(trans\text{-}CH=CHPh)((mim)_3COH)\}^+Cl^-]$.

3. Conclusions

Ruthenium(II) and osmium(II) complexes containing tridentate ligands tris(*N*-methylimidazol-2-yl)methanol and tris(*N*-ethoxymethylimidazol-2-yl)methanol were synthesised and characterised. Structures of $[\{RuCl(PPh_3)_2((mim)_3COH)\}^+Cl^-]$ (**2**) and

$[\{Ru(PPh_3)(CO)H((emim)_3COH)\}^+Cl^-]$ (**3b**) were determined by X-ray crystallography and showed that the structures of the complexes were similar to those of related Ru complexes containing tris(pyrazol-1-yl)borate ligands and tris(pyrazol-1-yl)methane ligands. The complex $[\{RuCl(PPh_3)_2((mim)_3COH)\}^+Cl^-]$ (**2**), with two triphenylphosphine groups in *cis* coordination sites, exhibits dynamic NMR behaviour consistent with interaction between the triphenylphosphine groups which gives rise to restricted rotation about the Ru–P bonds.

The ruthenium monohydride complex $[\{Ru(PPh_3)(CO)H((mim)_3COH)\}^+Cl^-]$ (**3a**) adds to the terminal C–H of acetylenes to reduce the acetylene and form a ruthenium alkenyl complex.

4. Experimental

4.1. Materials and measurements

All synthetic manipulations involving air sensitive materials were carried out under an inert atmosphere of argon in an argon filled dry-box or under a nitrogen atmosphere using standard Schlenk techniques. THF and hexane were dried over sodium before distillation from sodium and benzophenone under nitrogen. Ethanol and methanol were distilled from magnesium under nitrogen. *N*-methylimidazole (Aldrich) was used without further purification, *n*-butyllithium was titrated immediately prior to use against 2,5-dimethoxybenzyl alcohol [27].

^1H, ^{13}C and ^{31}P were recorded on a Bruker AMX400 or AMX600 spectrometer at 300 and 303 K respectively. ^1H and ^{13}C chemical shifts were internally referenced to residual solvent resonances. ^{31}P spectra were referenced to external neat trimethyl phosphite at 140.85 ppm. Infrared spectra were recorded on a Perkin–Elmer 1600 series FTIR; all frequencies are quoted in cm^{-1}. Melting points were recorded on a Reichert heating stage and are uncorrected. Mass spectra of organic compounds were recorded on a KRATOS MS9/MS50 double focusing mass spectrometer. Mass spectra of organometallic complexes were recorded on a Finnigan MAT TSQ-46 mass spectrometer (San Jose, CA). Data is quoted in the form $x(y)$ where x is the mass/charge ratio and y is the percentage abundance relative to the base peak. In the case of organometallic complexes in which the overall mass spectrum is predominantly that of the ligands, mass spectra were recorded scanning mass ranges greater than that of the free ligand, typically $m/z > 250$.

Tetrakis(triphenylphosphine)dichlororuthenium(II) [28], hydridocarbonylchlorotris(triphenylphosphine)-ruthenium(II) [29] and $[RuCl(PPh_3)_2(CO)(trans\text{-}HC{=}CHPh)]$ [30] were synthesised by literature methods. Hydridocarbonylchlorotris(triphenylphosphine)-osmium(II) was synthesised from ammonium hexachloroosmate in 84% yield [31].

4.1.1. Crystal structure determination

The crystallographic data for **2** and **3b** are summarised in Table 1. Cell constants were determined by a least-squares fit to the setting parameters of 25 independent reflections, measured and refined on an Enraf–Nonius CAD4-F diffractometer fitted with a graphite monochromator. Lorentz, polarisation and numerical absorption corrections were applied using the SDP system [32]. The structures were solved by direct methods using SHELXS-86 [33]. Refinement was performed by full-matrix least-squares methods using SHELX-76 [34]. The non-hydrogen atoms were refined anisotropically and hydrogen atoms were either included at calculated sites (C–H, N–H 0.97 Å) or located and refined with bond distance constraints (O–H 0.87 Å). Graphics were produced using ORTEP [35].

4.2. Synthesis of ligands

4.2.1. Tris(N-methylimidazol-2-yl)methanol (1) ((mim)$_3$COH)

Tris(*N*-methylimidazol-2-yl)methanol (**1**) $((mim)_3COH)$ was synthesised using a modification of the method reported by Tang et al. [17].

n-Butyllithium (44 mmol) was added to *N*-methylimidazole (6.6 ml, 83 mmol) in THF (100 ml) under nitrogen at −78 °C. The mixture was stirred at −78 °C for 1 h before addition of diethyl carbonate (3 ml, 25 mmol). The mixture was allowed to warm to room temperature over several hours. Water (50 ml) was added and the product was obtained by continuous liquid–liquid extraction with ethyl acetate (250 ml) overnight. The solvent was removed under vacuum and the residue was washed with acetone (30 ml) to give tris(*N*-methylimidazol-2-yl)methanol $((mim)_3COH)$ (**1a**) as a white crystalline solid (3.5 g, 87%); m.p. 190–191.5 °C (lit. 177.5–179.5 °C) [17]. ^1H NMR ($CDCl_3$): δ 6.89 (s, 6H, Ar–H), 3.42 (s, 9H, CH_3). $^{13}C\{^1H\}$ NMR ($CDCl_3$): δ 146.8 (*C2*), 127.0 (*C5*), 124.3 (*C4*), 72.2 (*C*–OH), 34.7 (CH_3).

4.2.2. Tris(N-ethoxymethylimidazol-2-yl)methanol (1b) ((emim)$_3$COH)

Tris(*N*-ethoxymethylimidazol-2-yl)methanol (**1b**) $((emim)_3COH)$ was synthesised using a modification of the method reported by Tang et al. [17].

n-Butyllithium (30 mmol) was added to *N*-ethoxymethylimidazole (6.5 g, 52 mmol) in THF (100 ml) under nitrogen at −78 °C. The mixture was stirred at −78 °C for 1 h before addition of diethyl carbonate (2 ml, 16.5 mmol). The mixture was allowed to warm to room temperature over several hours. Water (50 ml) was

added and the product was obtained by continuous liquid–liquid extraction with ethyl acetate. The solvent was removed under vacuum and the residue was recrystallised from acetone to give tris(*N*-ethoxymethylimidazol-2-yl)methanol (**1b**) ((emim)$_3$COH) as a white crystalline solid (1.9 g, 47%); m.p. 108–110 °C (lit. 101–103 °C) [17]. ^{1}H NMR ($CDCl_3$): δ 7.17 (d, $^3J_{H4-H5}$ = 1.4 Hz, 1H, *H4*), 6.96 (d, $^3J_{H5-H4}$ = 1.4 Hz, 1H, *H5*), 5.24 (s, 2H, N–CH_2), 3.26 (q, $^3J_{CH2-CH3}$ = 7.0 Hz, 2H, CH_2), 1.04 (t, $^3J_{CH3-CH2}$ = 7.0 Hz, 3H, CH_3). ^{13}C{^{1}H} NMR ($CDCl_3$): δ 146.8 (*C2*), 127.4 (*C4*), 121.8 (*C5*), 78.0 (N–CH_2), 72.7 (*C*–OH), 64.9 (CH_2), 16.1 (CH_3).

4.3. Synthesis of ruthenium complexes

4.3.1. [{RuCl(PPh$_3$)$_2$((mim)$_3$COH)}$^+$Cl$^-$] (2)

A mixture of Tetrakis(triphenylphosphine)dichlororuthenium(II) (0.60 g, 0.49 mmol) and (mim)$_3$COH (0.20 g, 0.74 mmol) in THF (40 ml) was stirred at room temperature for 2 h. The olive green solution was filtered and evaporated to dryness. The residue was extracted into ethanol (60 ml) and the volume reduced to 5–10 ml. [{RuCl(PPh$_3$)$_2$((mim)$_3$COH)}$^+$Cl$^-$] (**2**) formed as a yellow microcrystalline precipitate (0.14 g, 29%) which was filtered and washed with hexane; m.p. > 200 °C (decomposes without melting). ^{1}H NMR (400 MHz, methanol-d_4): δ 7.49–7.26 (m, 30H, *PPh$_3$*), 6.70 (s, 2H, *H4$_{A\ and\ C}$*), 6.43 (s, 2H, *H5$_{A\ and\ C}$*), 6.32 (d, 1H, $^3J_{H4B-H5B}$ = 1.5 Hz, *H4$_B$*), 4.79 (d, 1H, $^3J_{H5B-H4B}$ = 1.5 Hz, *H5$_B$*), 4.27 (s, 3H, N–CH_{3B}), 4.22 (s, 6H, N–C$H_{3A\ and\ C}$). ^{13}C{^{1}H} NMR (100 MHz, methanol-d_4): δ 144.2 (*C2$_{A\ and\ C}$*), 143.9 (*C2$_B$*), 136.7 (d, $^1J_{C-P}$ = 38.0 Hz, *ipso*-P*Ph$_3$*), 136.7 (*C5$_B$*), 136.0 (P*Ph$_3$*), 135.8 (*C4$_B$*), 133.1 (*C4$_{A\ and\ C}$*), 130.8 (P*Ph$_3$*), 129.0 (P*Ph$_3$*), 124.1 (*C5$_{A\ and\ C}$*), 79.5 (*C*–OH), 38.1 (N–*C*H$_{3B}$), 37.4 (N–*C*H$_{3A\ and\ C}$). ^{31}P{^{1}H} NMR (162 MHz, methanol-d_4): δ 41.3 (s). FAB MS *m*/*z* (%): 934 (4, (M + 2)$^+$), 933 (9, (M + 1)$^+$), 932 (4, M$^+$), 899 (26), 898 (20), 897 (32), 896 (17), 895 (22), 737 (20), 673 (19), 672 (12), 671 (28), 670 (19), 669 (13), 645 (37), 637 (17), 636 (19), 635 (24), 634 (20), 632 (12), 602 (14), 587 (12), 585 (17), 583 (13), 557 (14), 556 (28), 555 (43), 554 (19), 553 (100), 552 (22), 551 (37), 550 (13), 549 (13), 547 (15), 535 (12), 521 (15), 520 (20).

Crystal data. Crystals of **2** are yellow, triclinic prisms. The crystal data for **2** are summarised in Table 1. The atom numbering scheme is given in Fig. 2. Anal. Found: C, 59.6; H, 5.2; N, 8.5. $C_{49}H_{46}N_6OP_2RuCl_2 \cdot H_2O$ Calc.: C, 59.64; H, 4.90; N, 8.52%.

4.3.2. [{Ru(PPh$_3$)(Co)H((mim)$_3$COH)}$^+$Cl$^-$] (3a)

A mixture of [Ru(PPh$_3$)$_3$(CO)HCl] (0.50 g, 0.53 mmol) and (mim)$_3$COH (**1a**) (0.25 g, 0.92 mmol) in toluene (25 ml) was refluxed under nitrogen for 30 min. The reaction mixture was allowed to cool and the yellow precipitate which formed was isolated and washed with hexane (20 ml). The residue was recrystallized from methanol to yield [{Ru(PPh$_3$)(CO)H((mim)$_3$COH)}$^+$Cl$^-$] (**3a**) as a white solid (0.24 g, 65%); m.p. > 200 °C (decomposed without melting). ^{1}H NMR (600 MHz, methanol-d_4): δ 7.40–7.25 (m, 15H, P*Ph$_3$*), 7.12 (s, 1H, *H5$_A$*), 6.94 (s, 1H, *H4$_A$*), 6.86 (s, 1H, *H5$_B$*), 6.56 (s, 1H, *H5$_C$*), 6.03 (s, 1H, *H4$_B$*), 5.78 (s, 1H, *H4$_C$*), 4.03 (s, 3H, N–CH_{3B}), 3.99 (s, 3H, N–CH_{3A}), 3.94 (s, 3H, N–CH_{3C}), –12.06 (d, 1H, $^2J_{H-Ru-P}$ = 25.2 Hz, Ru–*H*). ^{13}C{^{1}H} NMR (100 MHz, methanol-d_4): δ 207.8 (d, $^2J_{C-Ru-P}$ = 18.1 Hz, Ru–*C*O), 144.9, 144.7, 144.5 (*C2$_{A,\ B\ and\ C}$*), 136.6 (d, $^1J_{C-P}$ = 45.1 Hz, *ipso*-P*Ph$_3$*), 135.4 (d, $^3J_{C-P}$ = 10.5 Hz, P*Ph$_3$*), 133.5 (*C4$_A$*), 131.5 (*C4$_C$*), 129.5 (d, $^2J_{C-P}$ = 9.5 Hz, P*Ph$_3$*), 129.5 (*C4$_B$*), 126.0 (*C5$_B$*), 125.3 (*C5$_A$*), 125.0 (*C5$_C$*), 37.6 (N–*CH$_{3B\ and\ C}$*), 37.1 (N–*CH$_{3A}$*). ^{31}P{^{1}H} NMR (162 MHz, methanol-d_4): δ 67.8 (s).

IR (Nujol, cm^{-1}): 1974.6 (w, Ru–H), 1922.1 (m, Ru–*C*≡*O*). FAB MS *m*/*z* (%): 669 (11, (M + 4)$^+$), 667 (71, (M + 3)$^+$), 665 (100, (M + 2)$^+$), 664 (34, (M + 1)$^+$), 663 (54, M$^+$), 662 (65), 660 (10), 659 (18), 584 (20), 583 (50), 582 (48), 581 (77), 580 (75), 579 (48), 578 (38), 577 (14), 575 (13), 556 (16), 555 (24), 554 (33), 553 (45), 552 (36), 551 (29), 550 (20), 405 (21). Anal. Found: C, 54.6; H, 4.7; N, 12.0. $C_{32}H_{32}N_6PO_2RuCl$ Calc.: C, 54.90; H, 4.61; N, 12.00%.

4.3.3. [{Ru(PPh$_3$)(CO)H((emim)$_3$COH)}$^+$Cl$^-$] (3b)

A mixture of [Ru(PPh$_3$)$_3$(CO)HCl] (0.50 g, 0.56 mmol) and (emim)$_3$COH (**1b**) (0.26 g, 0.64 mmol) in toluene (25 ml) was refluxed under nitrogen for 1 h. The reaction mixture was allowed to cool and the precipitate which formed was isolated and washed with hexane to yield the product [{Ru(PPh$_3$)(CO)H((emim)$_3$COH)}$^+$Cl$^-$] (**3b**) as a white solid (0.29 g, 66%); m.p. > 200 °C (decomposes without melting). ^{1}H NMR (600 MHz, methanol-d_4): δ 7.65–7.49 (m, 16H, P*Ph$_3$* and *H4$_A$*), 7.46 (s, 1H, *H5$_A$*), 7.33 (d, 1H, $^3J_{H5B-H4B}$ = 1.6 Hz, *H5$_B$*), 7.03 (d, 1H, $^3J_{H5C-H4C}$ = 1.6 Hz, *H5$_C$*), 6.39 (d, 1H, $^3J_{H4B-H5B}$ = 1.6 Hz, *H4$_B$*), 6.13 (s, 1H, $^3J_{H4C-H5C}$ = 1.6 Hz, *H4$_C$*), 6.08 (d, 1H, $^2J_{H-C-H}$ = 10.1 Hz, CH_{2B}), 5.98 (d, 1H, $^2J_{H-C-H}$ = 10.4 Hz, CH_{2C}), 5.93 (dd, $^2J_{H-C-H}$ = 10.4 Hz, 2H, N–CH_{2A}), 5.85 (d, 1H, $^2J_{H-C-H}$ = 10.1 Hz, N–CH_{2B}), 5.76 (d, $^2J_{H-C-H}$ = 10.4 Hz, 1H, N–CH_{2C}), 3.84–3.81 (m, 2H, $^3J_{CH2-CH3}$ = 7.3 Hz, N–CH_{2B}), 3.77–3.71 (m, 4H, $^3J_{CH2-CH3}$ = 7.3 Hz, N–C$H_{2A\ and\ C}$), 1.38 (t, 3H, $^3J_{CH3-CH2}$ = 7.2 Hz, CH_{3B}), 1.35 (t, 3H, $^3J_{CH3-CH2}$ = 7.2 Hz, CH_{3C}), 1.29 (t, 3H, $^3J_{CH3-CH2}$ = 7.3 Hz, CH_{3A}), –11.75 (d, 1H, $^2J_{H-Ru-P}$ = 25.0 Hz, Ru–*H*). ^{13}C{^{1}H} NMR (100 MHz, methanol-d_4): δ 207.5 (d, $^2J_{C-Ru-P}$ = 18.1 Hz, Ru–*C*O), 144.8 (*C2$_B$*), 144.3 (*C2$_{A\ and\ C}$*), 136.2 (d, $^1J_{C-P}$ =

45.1 Hz, *ipso*-PPh_3), 135.3 (d, $^2J_{C-P}$ = 10.5 Hz, PPh_3), 133.2 ($C5_A$), 132.3 ($C4_C$), 131.7 (PPh_3), 131.4 ($C4_B$), 129.7 (d, $^3J_{P-C}$ = 9.8 Hz, PPh_3), 124.9 ($C5_B$), 124.7 ($C4_A$), 123.8 ($C5_C$), 79.3 (N–$CH_{2A\ and\ C}$), 79.2 (N–CH_{2B}), 66.9 (CH_{3B}), 66.8 ($CH_{3A\ and\ C}$). $^{31}P\{^1H\}$ NMR (162 MHz, methanol-d_4): δ 66.6 (s).

IR (Nujol, cm^{-1}): 1989.0 (w, Ru–H), 1920.8 (m, Ru–$C{\equiv}O$). FAB MS *m/z* (%): 800 (46, $(M+4)^+$), 799 (55, $(M+3)^+$), 798 (78, $(M+2)^+$), 797 (100, $(M+1)^+$), 796 (69, M^+), 794 (93), 791 (18), 672 (11), 671 (28), 670 (28), 669 (30), 668 (19), 666 (20), 644 (14), 643 (20), 642 (10), 641 (36), 640 (15), 567 (13), 537 (14), 536 (11), 535 (24), 534 (18), 533 (13), 531 (14). Anal. Found: C, 53.5; H, 5.5; N, 9.9. $C_{38}H_{44}N_6O_5PRuCl \cdot H_2O$ Calc.: C, 53.68; H, 5.45; N, 9.88%.

Crystal data. Crystals of **3b** are colourless, triclinic prisms. The crystal data for **3b** are summarised in Table 1. The atom numbering scheme is given in Fig. 3.

4.3.4. [{Os(PPh_3)(CO)H((mim)$_3$COH)}$^+$Cl$^-$] (4a)

A mixture of [Os(PPh_3)$_3$(CO)HCl] (0.25 g, 0.24 mmol) and (mim)$_3$COH (**1a**) (0.08 g, 0.30 mmol) in toluene (40 ml) was refluxed under nitrogen for 1 h. After 10–15 min, the colour of the solution changed to deep red. The solvent was removed and the residue was extracted with methanol. The methanol solution was filtered and evaporated to dryness. The residue was washed with hexane and dried to yield [{Os(PPh_3)(CO)H((mim)$_3$COH)}$^+$Cl$^-$] (**4a**) as a cream solid (0.14 g, 74%); m.p. > 200 °C (decomposed without melting). ^1H NMR (600 MHz, methanol-d_4): δ 7.58–7.47 (m, 16H, PPh_3 and $H4_A$), 7.18 (s, 1H, $H5_A$), 7.09 (d, 1H, $^3J_{H5B-H4B}$ = 1.4 Hz, $H5_B$), 6.75 (d, 1H, $^3J_{H5C-H4C}$ = 1.5 Hz, $H5_C$), 6.35 (d, 1H, $^3J_{H4B-H5B}$ = 1.4 Hz, $H4_B$), 6.09 (d, 1H, $^3J_{H4C-H5C}$ = 1.5 Hz, $H4_C$), 4.29 (s, 3H, N–CH_{3B}), 4.25 (s, 3H, N–CH_{3A}), 4.19 (s, 3H, N–CH_{3C}), −12.90 (d, 1H, $^2J_{H-M-P}$ = 18.0 Hz, Os–*H*). $^{13}C\{^1H\}$ NMR (100 MHz, methanol-d_4): δ 188.4 (d, $^2J_{C-Os-P}$ = 11.0 Hz, Os–*C*O), 143.7, 142.8, 142.6 ($C2_{A,\ B\ and\ C}$), 137.0 (d, $^1J_{C-P}$ = 51.1 Hz, *ipso*-PPh_3), 135.1 (d, $^2J_{C-P}$ = 10.2 Hz, PPh_3), 134.1 ($C4_A$), 132.8 ($C4_C$), 131.7 ($C4_B$), 131.2 (PPh_3), 129.1 (d, $^3J_{C-P}$ = 9.3 Hz, PPh_3), 126.2 ($C5_B$), 125.7 ($C5_A$), 125.1 ($C5_C$), 37.5 (N–CH_{3B}), 37.3 (N–CH_{3A}), 36.9 (N–CH_{3C}). $^{31}P\{^1H\}$ NMR (162 MHz, methanol-d_4): δ 26.1 (s).

IR (Nujol, cm^{-1}): 2063.8 (w, Os–H), 1880.5 (m, Os–$C{\equiv}O$). FAB MS *m/z* (%): 756 (21, $(M+2)^+$), 755 (91, $(M+1)^+$), 753 (100, M^+), 751 (52), 749 (15), 673 (16), 672 (26), 671 (77), 669 (41), 668 (22), 667 (24), 657 (17), 655 (13), 654 (12), 653 (12), 642 (10).

4.3.5. [{Os(PPh_3)(CO)H((emim)$_3$COH)}$^+$Cl$^-$] (4b)

A mixture of [Os(PPh_3)$_3$(CO)HCl] (0.25 g, 0.24 mmol) and (emim)$_3$COH (**1b**) (0.11 g, 0.27 mmol) in toluene (40 ml) was refluxed under nitrogen for 3 h. After 10–15 min the colour of the solution changed to deep red/brown. After 3 h, the solvent was removed and the product extracted with methanol. The methanol solvent was removed leaving a red viscous solid which was dissolved in isopropanol. On slow addition of hexane a cream solid precipitated, which was collected, washed with hexane and dried. [{Os(PPh_3)(CO)H((emim)$_3$COH)}$^+$Cl$^-$] (**4b**) was obtained as a cream solid (0.13 g, 59%); m.p. > 200 °C (decomposed without melting). ^1H NMR (600 MHz, methanol-d_4): δ 7.64–7.52 (m, 17H, PPh_3, $H4_A$ and $H5_A$), 7.41 (d, 1H, $^3J_{H5B-H4B}$ = 1.3 Hz, $H5_B$), 7.05 (d, 1H, $^3J_{H5C-H4C}$ = 1.7 Hz, $H5_C$), 6.45 (d, 1H, $^3J_{H4B-H5B}$ = 1.3 Hz, $H4_B$), 6.19 (d, 1H, $^3J_{H4C-H5C}$ = 1.7 Hz, $H4_C$), 6.12 (d, 1H, $^2J_{H-C-H}$ = 10.6 Hz, N–CH_{2B}), 6.02 (d, 1H, $^2J_{H-C-H}$ = 10.2 Hz, N–CH_{2C}), 5.96 (ABq, 2H, $^2J_{H-C-H}$ = 10.2 Hz, N–CH_{2A}), 5.87 (d, 1H, $^2J_{H-C-H}$ = 10.6 Hz, N–CH_{2B}), 5.75 (d, 1H, $^2J_{H-C-H}$ = 10.2 Hz, N–CH_{2C}), 3.88–3.83 (m, 2H, $^3J_{CH2-CH3}$ = 7.2 Hz, CH_{2B}), 3.78–3.73 (m, 4H, $^3J_{CH2-CH3}$ = 7.2 Hz, C$H_{2C\ and\ A}$), 1.39 (t, 3H, $^3J_{CH3-CH2}$ = 7.2 Hz, CH_{3B}), 1.36 (t, 3H, $^3J_{CH3-CH2}$ = 7.2 Hz, CH_{3C}), 1.29 (t, 3H, $^3J_{CH3-CH2}$ = 7.2 Hz, CH_{3A}), −12.73 (d, 1H, $^2J_{H-Os-P}$ = 18.0 Hz, Os–*H*). $^{13}C\{^1H\}$ NMR (100 MHz, methanol-d_4): δ 188.0 (d, $^2J_{C-P}$ = 11.8 Hz, Os–*C*O) 143.6, 142.4, 142.2 ($C2_{A,\ B\ and\ C}$), 136.6 (d, $^1J_{C-P}$ = 51.1 Hz, *ipso*-PPh_3), 135.1 (d, $^2J_{C-P}$ = 10.5 Hz, PPh_3), 134.2 ($C4_A$ and $C5_A$), 132.8 ($C4_C$), 131.9 ($C4_B$), 131.4 (s, PPh_3), 129.4 (d, $^3J_{P-C}$ = 10.0 Hz, PPh_3), 125.02 ($C5_B$), 123.9 ($C5_C$), 79.1 (N–CH_{2B}), 79.0 (N–$CH_{2A\ and\ C}$), 66.9 (CH_{2B}), 66.8 (CH_{2C}), 66.7 (CH_{2A}), 15.4 (CH_{3B}), 15.3 ($CH_{3A\ and\ C}$). $^{31}P\{^1H\}$ NMR (162 MHz, methanol-d_4): δ 25.6 (s).

IR (Nujol, cm^{-1}): 2062.5 (w, Os–H), 1895.8 (m, Os–$C{\equiv}O$). FAB MS *m/z* (%): 889 (17, $(M+4)^+$), 888 (27, $(M+3)^+$), 887 (100, $(M+2)^+$), 886 (22, $(M+1)^+$), 885 (64, M^+), 884 (67), 883 (58), 881 (19), 837 (19), 835 (22), 833 (20), 761 (28), 760 (31), 759 (76), 757 (46), 756 (23), 755 (22), 746 (24), 745 (49), 744 (32), 743 (44), 742 (42), 741 (27), 740 (19), 733 (19), 731 (20), 715 (19), 701 (23), 571 (23), 555 (22), 553 (29), 541 (24), 525 (28), 511 (23), 509 (23).

4.3.6. [{Ru(PPh_3)(CO)(*trans*-HC=CHPh)((mim)$_3$COH)}$^+$Cl$^-$] (5)

4.3.6.1. Reaction of phenylacetylene with [{Ru(PPh_3)(CO)H((mim)$_3$COH)}$^+$Cl$^-$] (3a). Phenylacetylene (0.1 ml) was added to a solution of [{Ru(PPh_3)(CO)H((mim)$_3$COH)}$^+$Cl$^-$] (**3a**) (25 mg, 0.33 mmol) in methanol-d_4 (0.5 ml) in an NMR tube. The tube was heated in an oil bath at 40 °C and the reaction monitored by ^{31}P NMR. After 2 days no starting complex remained by ^{31}P NMR. The volatiles were removed under vacuum and the residue was recrys-

tallised from acetone. The major product obtained was that in which the phenylacetylene was converted to the alkenyl complex **5**. The compound was identical to an authentic sample prepared by the reaction of $[RuCl(PPh_3)_2(CO)(trans\text{-}HC{=}CHPh)]$ with $(mim)_3COH$.

^1H NMR (600 MHz, $CDCl_3$): δ 9.61 (s, 1H, CO*H*), 7.99 (dd, 1H, $^3J_{H-C=C-H}$ = 17.0 Hz, $^3J_{HC-Ru-P}$ = 2.0 Hz, Ru*H*C=C), 7.30 (m, 3H, *p*-PPh_3), 7.22–7.15 (m, 12H, *o*-PPh_3, *m*-PPh_3), 7.11 (t, 2H, $^3J_{H-H}$ = 7.6 Hz, *m*-CH*Ph*), 7.02 (m, 2H, *m*-CH*Ph*), 7.02 (s, 1H, $H4_C$), 6.91 (t, 1H, $^3J_{H-H}$ = 7.0 Hz, *p*-CH*Ph*), 6.48 (s, 1H, $H5_C$), 6.40 (d, 1H, $^3J_{H4B-H5B}$ = 1.3 Hz, $H4_B$), 6.38 (d, 1H, $^3J_{H4A-H5A}$ = 1.3 Hz, $H4_A$), 6.24 (d, 1H, $^3J_{H-C=C-H}$ = 17.0 Hz, *H*C=C), 5.99 (d, 1H, $^3J_{H5A-H4A}$ = 1.3 Hz, $H5_A$), 5.95 (d, 1H, $^3J_{H5B-H4B}$ = 1.3 Hz, $H5_B$), 4.28 (s, 3H, N–CH_{3A}), 4.23 (s, 3H, N–CH_{3B}), 3.97 (s, 3H, N–CH_{3C}). $^{13}C\{^1H\}$ NMR (100 MHz, $CDCl_3$): δ 206.8 (d, $^2J_{C-Ru-P}$ = 16.3 Hz, Ru–*C*O), 161.4 (d, $^2J_{C-P}$ = 12.8 Hz, *C*H=CHPh), 144.3, 143.7, 143.6, 142.1 ($C2_{A, B \text{ and } C}$ and ^iCH*Ph*), 137.6 (CH=*C*HPh), 134.8 (d, $^3J_{C-P}$ = 9.8 Hz, PPh_3), 133.0 (d, $^1J_{C-P}$ = 43.2 Hz, *ipso*-PPh_3), 130.7 (PPh_3), 130.6 ($C4_C$), 130.5 ($C5_B$), 128.8 (d, J_{C-P} = 9.4 Hz, PPh_3), 128.8 (*m*-CH=*Ph*), 128.5 ($C5_C$), 124.9 (*o*-CH=*Ph*, *p*-CH=*Ph*), 124.8 ($C5_B$), 124.5 ($C4_A$), 123.1 ($C5_C$), 78.4 (*C*–OH), 39.4 (N–CH_{3A}), 39.0 (N–CH_{3B}), 37.1 (N–CH_{3C}). $^{31}P\{^1H\}$ NMR (162 MHz, $CDCl_3$): δ 50.09 (s).

IR (Nujol, cm^{-1}): 1926.7 (m, Ru–*C*≡*O*). FAB MS *m*/*z* (%): 770 (18, $(M+4)^+$), 769 (64, $(M+3)^+$), 768 (23, $(M+2)^+$), 767 (100, $(M+1)^+$), 766 (41, M^+), 765 (48), 764 (31), 761 (22), 667 (17), 666 (20), 665 (73), 662 (37), 661 (33), 660 (32), 657 (23), 635 (32), 633 (20), 585 (18), 584 (24), 583 (52), 582 (37), 581 (73), 580 (42), 579 (36), 578 (34), 575 (19), 567 (19), 556 (25), 555 (33), 551 (36), 550 (25), 547 (17), 507 (20), 506 (20).

4.3.6.2. Preparation of an authentic sample of $[\{Ru(PPh_3)(CO)(trans\text{-}HC{=}CHPh)((mim)_3COH)\}^+Cl^-]$ **(5)**. Tris(*N*-methylimidazol-2-yl)methanol ($(mim)_3COH$) (**1a**) (50 mg, 0.18 mmol) was added to a stirred solution of $[RuCl(PPh_3)_2(CO)(trans\text{-}HC{=}CHPh)]$ (100 mg, 0.13 mmol) in toluene (30 ml) under nitrogen. The colour of the solution disappeared within 5 min. The solution was stirred overnight and the precipitate which formed was isolated by filtration and washed with light petroleum. $[\{Ru(PPh_3)(CO)(HC{=}CHPh)((mim)_3COH)\}^+Cl^-]$ (**5**) was obtained as a cream solid (90 mg, 89%).

5. Supplementary material available

Listings of atom coordinates, anisotropic thermal parameters, torsion angles, details of least-squares planes calculations (61 pages) for **2** and **3b**. Ordering information is given on any current masthead page.

Acknowledgements

We gratefully acknowledge financial support from the Australian Research Council.

References

[1] L.K. Thompson, B.S. Ramaswamy and E.A. Seymour, *Can. J. Chem., 55* (1977) 878.
[2] R.S. Brown, N.J. Curtis and J. Huguet, *J. Am. Chem. Soc., 103* (1981) 6953.
[3] F. Chu, J. Smith, V.M. Lynch and E.V. Anslyn, *Inorg. Chem., 34* (1995) 5689.
[4] X-M. Chen, Z-T. Xu and T.C.W. Mak, *Polyhedron, 14* (1995) 319.
[5] S.M. Gorun, G.C. Papaefthymiou, R.B. Frankel and S.J. Lippard, *J. Am. Chem. Soc., 109* (1987) 4244.
[6] W.B. Tolman, S. Liu, J.G. Bentsen and S.J. Lippard, *J. Am. Chem. Soc., 113* (1991) 152.
[7] S.J. Lippard, *Angew. Chem., Int. Ed. Engl., 27* (1988) 344.
[8] T.N. Sorrell, W.E. Allen and P.S. White, *Inorg. Chem., 34* (1995) 952.
[9] N. Wei, N.N. Murthy, Z. Tyeklár and K.D. Karlin, *Inorg. Chem., 33* (1994) 1177.
[10] T.N. Sorrell, *Tetrahedron, 45* (1989) 3.
[11] P.K. Byers, A.J. Canty, L.M. Engelhardt, J.M. Patrick and A.H. White, *J. Chem. Soc., Dalton Trans.*, (1995) 981.
[12] W.B. Tolman, R.L. Rardin and S.J. Lippard, *J. Am. Chem. Soc., 111* (1989) 4532.
[13] T.G. Traylor, K.W. Hill and Z-Q. Tian, *J. Am. Chem. Soc., 110* (1988) 5571.
[14] P.K. Byers, A.J. Canty and R.T. Honeyman, *J. Organomet. Chem., 385* (1990) 417; P.K. Byers and A.J. Canty, *Organometallics, 9* (1990) 210; P.K. Byers and A.J. Canty, *J. Chem. Soc., Chem. Commun.*, (1988) 639; P.K. Byers, A.J. Canty, B.W. Skelton and A.H. White, *Organometallics, 9* (1990) 826; G.B. Brown, P.K. Byers and A.J. Canty, *Organometallics, 9* (1990) 1231.
[15] M.J. Bloemink, H. Engelking, S. Karentzopoulos, B. Krebs and J. Reedijk, *Inorg. Chem., 35* (1996) 619.
[16] A.J. Canty, P.R. Traill, B.W. Skelton and A.H. White, *Inorg. Chim. Acta*, in press.
[17] C.C. Tang, D. Davilian, P. Huang and R.J. Breslow, *J. Am. Chem. Soc., 100* (1978) 3918.
[18] N.W. Alcock, I.D. Burns, K.S. Claire and A.F. Hill, *Inorg. Chem., 31* (1992) 2906.
[19] L.P. Soler, B.A. Messerle, L. Field and T.W. Hambley, unpublished results, 1996.
[20] A. Llobet, D.J. Hodgson and T.J. Meyer, *Inorg. Chem., 29* (1990) 3760.
[21] M. Fajardo, A. de la Hoz, E. Diéz-Barra, F.A. Jalón, A. Otero, A. Rodríguez, J. Tejeda, D. Belletti, M. Lanfranchi and M.A. Pellinghelli, *J. Chem. Soc., Dalton Trans.*, (1993) 1935.
[22] N-Y. Sun and S.J. Simpson, *J. Organomet. Chem., 434* (1992) 341.
[23] S.G. Davies, A.E. Derome and J.P. McNally, *J. Am. Chem. Soc., 113* (1991) 2854; F.P. Fanizzi, M. Lanfranchi, G. Natile and A. Tiripicchio, *Inorg. Chem., 33* (1994) 3331; C.H. Bushweller, C.D. Rithner and D. Butcher, *Inorg Chem., 25* (1986)

1610; G. Hunter, T.J.R. Weakley and W. Weissensteiner, *J. Chem. Soc., Dalton Trans.*, (1987) 1545; B.E. Mann, C. Master, B.L. Shaw and R.E. Stainbank, *J. Chem. Soc. Chem. Commun.*, (1971) 1103.

[24] N.W. Alcock, A.F. Hill and R.P. Melling, *Organometallics, 10* (1991) 3898; A.F. Hill, *J. Organomet. Chem., 395* (1990) C35.

[25] H. Loumhari, J. Ros, M.R. Torres and A. Perales, *Polyhedron, 9* (1990) 907 and references cited therein.

[26] M.R. Torres, A. Santos, J. Ros and X. Solans, *Organometallics, 6* (1987) 1091; T. Blackmore, M.I. Bruce and F.G.A. Stone, *J. Chem. Soc., Dalton Trans.*, (1974) 106; H. Yamazaki and K. Aoki, *J. Organomet. Chem., 122* (1976) C54.

[27] J.M. Lansinger, R.C. Ronald and N.R. Winkle, *J. Chem. Soc., Chem. Commun.*, (1980) 87.

[28] T.A. Stephenson and G. Wilkinson, *J. Inorg. Nucl. Chem., 28* (1966) 945.

[29] N.J. Ahmad, J. Levison, S.D. Robinson and M.F. Uttley, *Inorg. Synth., 15* (1974) 48.

[30] M.R. Torres, A. Vegas and A. Santos, *J. Organomet. Chem., 309* (1986) 169.

[31] N.J. Ahmad, J. Levison, S.D. Robinson and M.F. Uttley, *Inorg. Synth., 15* (1974) 53.

[32] B.A. Frenz, SDP, *Enraf–Nonius Structure Determination Package*, Enraf–Nonius, Delft, Netherlands, 1985.

[33] G.M. Sheldrick, SHELX-86, in G.M. Sheldrick, C. Krüger and R. Goddard (eds.), *Crystallographic Computing 3*, Oxford University Press, Oxford, UK, 1986, pp. 175–189.

[34] G.M. Sheldrick, SHELX-76, *Program for Crystal Structure Determination*, University of Cambridge, Cambridge, UK, 1976.

[35] C.K. Johnson, ORTEP, *Report ORNL-3794*, Oak Ridge National Laboratory, Oak Ridge, TN, 1965.